Characterization of Cisplatin/Membrane Interactions by QM/MM Energy Decomposition Analysis

Gustavo Cárdenas,[†] Álvaro Pérez-Barcia,[‡] Marcos Mandado,[*,‡] and Juan J. Nogueira[*,†,¶]

†Department of Chemistry, Universidad Autónoma de Madrid, Calle Francisco Tomás y Valiente, 7, 28049, Madrid, Spain

‡Department of Physical Chemistry, University of Vigo, Lagoas-Marcosende s\n, ES-36310-Vigo, Galicia, Spain

¶IADCHEM, Institute for Advanced Research in Chemistry, Universidad Autónoma de Madrid, Calle Francisco Tomás y Valiente, 7, 28049 Madrid, Spain

E-mail: mandado@uvigo.es; juan.nogueira@uam.es

Abstract

The intermolecular interactions established between anticancer drugs and lipid membranes play a key role in the permeation mechanism of the drugs inside the cells. Herein we extend a quantum mechanical energy decomposition analysis scheme based on deformation electron densities to a hybrid multiscale electrostatic embedding quantum mechanics/molecular mechanics (QM/MM) framework, and apply it to characterize the interactions between the cisplatin drug and a dioleyl-phosphatidylcholine lipid membrane. The interaction energy decomposition into electrostatic, induction, dispersion and Pauli repulsion contributions is performed for ensembles of geometries

1

taken from molecular dynamics simulations to account for conformational sampling and, thus, obtain a distribution of each of the energy components. Contrary to a previous energy decomposition using force fields, it is evidenced that the electrostatic component is predominant in both polar and non-polar regions of the bilayer, and the repulsive component is strong when considered quantum mechanically, while being largely underestimated by the force field.

The permeation of drugs across cell membranes is a key biological process which largely determines the efficacy of the drugs.[1,2] In general, the transport of small and moderately polar molecules happens by passive diffusion through the lipid bilayer, while larger and more polar compounds enter the cell by active transport mediated by membrane proteins.[3,4] However, many species present intermediate size and polarity and, thus, can be uptaken by the cells through both mechanisms, as it is the case of platinum-based agents.[5–7] Platinum complexes are anticancer drugs employed in chemotherapy, whose cytotoxic mechanisms have been intensively investigated in the last decades.[8–13] Among these species, cis-diamminedichloroplatinum (II) (cisplatin) is the most frequently used compound to treat different types of human cancers.[14–17] The interaction between the drug and lipid membranes along the passive entrance of the compound inside cancer cells has shown to be fundamental in the mode of action of cisplatin, including the development of resistance mechanisms by some cancer cells[18,19] and the activation of apoptotic routes.[7,20] Therefore, the characterization of the interactions between cisplatin and the lipids that compose the cellular membranes is of great relevance to get fundamental insight into the membrane processes involved in the biological activity of cisplatin and other platinum agents.

The computer simulation of the transport of drugs through lipid membranes is usually carried out by a combination of classical molecular dynamics and enhanced-sampling approaches.[21–26] Specifically, the passive diffusion of cisplatin through different lipid bilayers has been investigated by umbrella sampling simulations.[27–30] Despite the significant mechanistic details obtained from the previous theoretical work, the nature of the drug/lipid

interactions has been barely characterized in terms of simple force field contributions.[30] However, a more realistic description requires the use of more accurate methodologies, such as quantum mechanical interaction energy partitioning schemes based on variational or perturbational approaches.[31–34] These methods provide different contributions to the total interaction energy, such as Pauli, electrostatic, induction and dispersion terms, some of them not properly described by neither fixed-charge nor polarizable force fields. However, such quantum mechanical approaches have not been widely applied to the investigation of biological systems mainly due to two reasons: (i) the computational cost associated to the calculation of the interaction energy for large systems, and (ii) the need to perform the calculations for ensembles of geometries in order to consider conformational sampling. Thus, energy decomposition analyses (EDA) are usually limited to the investigation of small molecular systems[35–37] or relatively large systems (few tens of atoms) within a static framework.[38–41] In line with these considerations, it becomes clear that a compromise between the computational cost and the level of theory implemented for the study of the interaction energies needs to be achieved, especially on the description of complex biological systems. Herein we characterized the interactions that drive the permeation of cisplatin through a dioleylphosphatidylcholine (DOPC) lipid membrane by means of a quantum mechanics/molecular mechanics (QM/MM) EDA approach. We focus our analysis on the minimum (Min) and the maximum (Max) of the free-energy profile (represented in Figure 1) previously computed by umbrella sampling molecular dynamics simulations.[30] The Min region is located at the interface between the polar heads and the non-polar tails of DOCP, while the Max region is at the center of the bilayer.
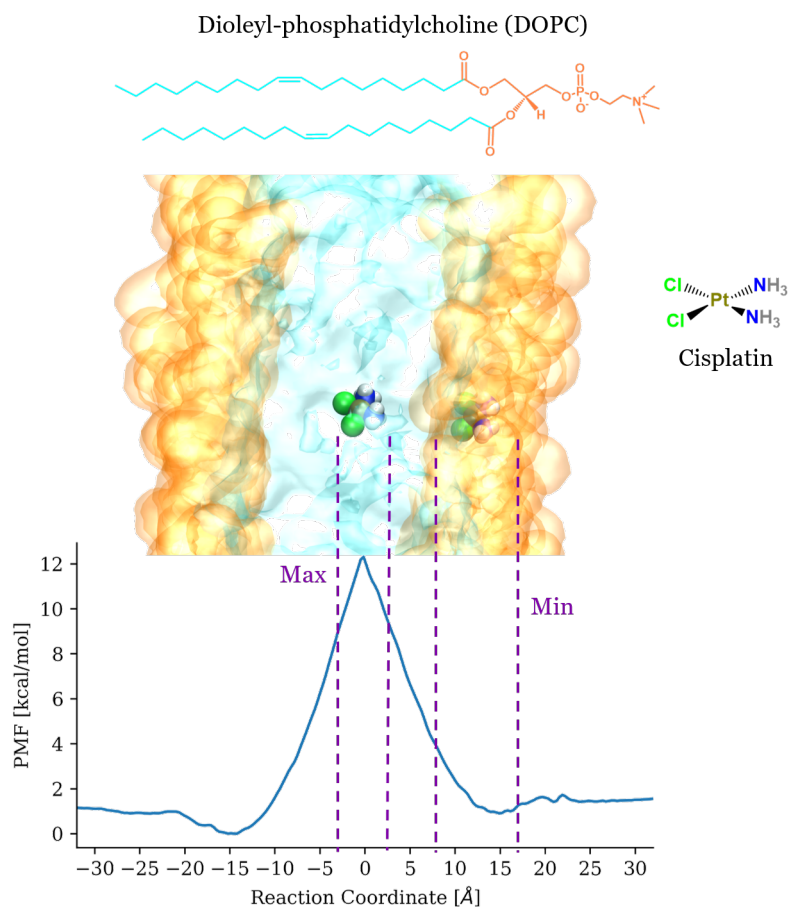
Figure 1: Top: Schematic representation of the cisplatin molecule embedded in a dioleyl-phosphatidylcholine lipid membrane. The polar and non-polar regions of the membrane are represented in orange and cyan, respectively. Bottom: Potential of mean force (PMF) profile of the permeation of cisplatin inside the lipid membrane[30] displaying the two regions (Min and Max) under study in the present work.

Our main goal is threefold: (i) to implement a QM/MM EDA able to treat large systems; (ii) to characterize the nature of each of the components of the cisplatin/membrane interaction energy on the Min and Max regions; and (iii) to evidence the importance of considering conformational sampling in the model.

The interaction energy between two fragments A and B of a molecular system is defined as the difference between the energy of the AB complex and the energies of the isolated A and B fragments.

$$E_{\text{int}} = E_{\text{AB}} - (E_{\text{A}}^{\text{AB}} + E_{\text{B}}^{\text{AB}}) \tag{1}$$

In Eq (1) the superscript AB indicates that the energies of A and B are calculated considering their geometries in the complex and the basis set of the complex. The latter is introduced to correct the basis set superposition error.[42]

In this work the system is divided into two subsystems, namely the cisplatin molecule on the one hand and the DOPC membrane plus the water molecules and the K^+ and Cl^- ions on the other hand; thus, in accordance with Eq (1), these subsystems correspond to the A and B moieties, respectively, and the AB complex is represented by the cisplatin molecule embedded in the solvated lipid membrane. Considering this division, we adopt an EDA scheme based on deformation electron densities, initially developed and implemented for quantum mechanical methods.[43,44] This methodology is based on the definition of the one-electron and the exchange-correlation unperturbed and deformation densities, the latter associated to Pauli and polarization effects. Thus, the one-electron density of the complex may be written as,

$$\rho(\mathbf{r}) = \rho_{\text{A}}(\mathbf{r}) + \rho_{\text{B}}(\mathbf{r}) + \Delta\rho_{\text{Pau}}(\mathbf{r}) + \Delta\rho_{\text{pol}}(\mathbf{r}) \tag{2}$$

where the first two terms in the rhs of Eq (2) are the unperturbed densities of the subsystems A and B and the last two terms correspond to the Pauli and polarization deformation

densities. In the same way, the exchange-correlation density of the complex may also be written as,

$$\rho_{\mathrm{XC}}(\mathbf{r_1}, \mathbf{r_2}) = \rho_{\mathrm{XC,A}}(\mathbf{r_1}, \mathbf{r_2}) + \rho_{\mathrm{XC,B}}(\mathbf{r_1}, \mathbf{r_2}) + \rho_{\mathrm{X,AB}}(\mathbf{r_1}, \mathbf{r_2}) + \Delta\rho_{\mathrm{XC}}(\mathbf{r_1}, \mathbf{r_2}) \tag{3}$$

where the first two terms represent contributions from the isolated subsystems and the last two terms from intermolecular electron exchange and polarization interactions, in this order. The definitions given by Eqs (2) and (3) allow for decomposing the total interaction energy into electrostatic, exchange, repulsion and polarization contributions,

$$E_{\mathrm{int}} = E_{\mathrm{elec}} + E_{\mathrm{exc}} + E_{\mathrm{rep}} + E_{\mathrm{pol}} \tag{4}$$

E_{exc} and E_{rep} together account for the traditional Pauli repulsion energy, E_{Pau}, whereas E_{pol} may be split into the second order induction energy, E_{ind}, and dispersion energy plus higher-order polarization terms, $E_{\mathrm{disp+res-pol}}$. In what follows we will refer to the latter term as dispersion energy, E_{dis}, because this is by far the dominant contribution. Thus, with the introduction of the perturbation expansion of the one-electron and exchange-correlation densities, one obtains the following partition,

$$E_{\mathrm{int}} = E_{\mathrm{elec}} + E_{\mathrm{Pau}} + E_{\mathrm{ind}} + E_{\mathrm{dis}} \tag{5}$$

It should be emphasized here that the lipid membrane is composed by 128 lipid chains formed by 138 atoms each, so that in practice only a part of the lipid membrane can be treated at a quantum mechanical level. In order to account for the presence of the remaining atoms an electrostatic-embedding QM/MM computational scheme has been adopted both in the computation of the interaction energy and in the EDA, where the classical charges of the environment polarize the QM region. A full derivation of the different energy terms given above is provided in the Supporting Information.

Due to the large size of the system investigated here it is necessary to analyze the con-

6

vergence of the interaction energy and its different contributions with respect to the size of the QM region and the number of sampled geometries considered in the calculations. For the first purpose, we randomly selected a geometry from a 15 ns molecular dynamics run in the Min region and in the Max region, and in each case we performed the QM/MM energy calculations and the EDA increasing the number of DOPC molecules in the QM region. Moreover, in order to investigate the effect of including the point charges of the classical environment in the EDA, the energy terms were obtained without (Figure 2a,b) and with (Figure 2c,d) point charges. It can be seen that for the calculations without point charges, the dispersion, induction and Pauli contributions converge after including at least 5 DOPC molecules in the QM region. However, the total interaction energy does not converge even for 7 DOPC molecules in the QM region, as can be evidenced from Figure 2a,b; this is due to the fact that the electrostatic contribution assumes an oscillatory behavior between 3 and 7 DOPC molecules. On the other hand, the counterpart calculations that include the point charges that surround the QM region (Figure 2c,d) display a good convergence for all the interaction energy terms after including 5 DOPC molecules in the QM region. These results suggest that although considering the entire system quantum mechanically is computationally unfeasible, it would still be necessary to include the polarizing effect of the surrounding environment by an electrostatic-embedding QM/MM approach. Furthermore, in the case of the system under study, it represents an excellent compromise to incorporate the cisplatin molecule plus 6 DOPC molecules to the QM region, and consider the remaining atoms as point charges in the MM region.

Next, we have investigated the convergence of the energies with the number of geometries. This is done by sampling 190 geometries from a previously performed[30] molecular dynamics simulation at the Min region, and 194 geometries from a molecular dynamics simulation at the Max region. For each of the sampled geometries, the EDA was performed considering the cisplatin molecule plus six DOPC molecules in the QM region, with overall 839 atoms treated quantum mechanically. In order to ensure that 190 (194) geometries are

an appropriate statistical ensemble, we analyzed the convergence of the energy components as the number of averaged geometries increases, selecting these geometries in an equidistant manner from the 190 (194) geometries of the Min (Max) region. As can be evinced from Figure 2e,f, the induction and the dispersion energies are mostly converged after considering 50 geometries. However, the convergence is most difficult to achieve for the electrostatic and Pauli components. The former is converged only after considering 100 geometries, and the latter still shows a slight increase when going from 100 to 190 geometries. This highlights the importance of including conformational sampling in the theoretical model. In the following analyses, the 190 (194) geometries sampled at the Min (Max) region of the membrane will be considered.
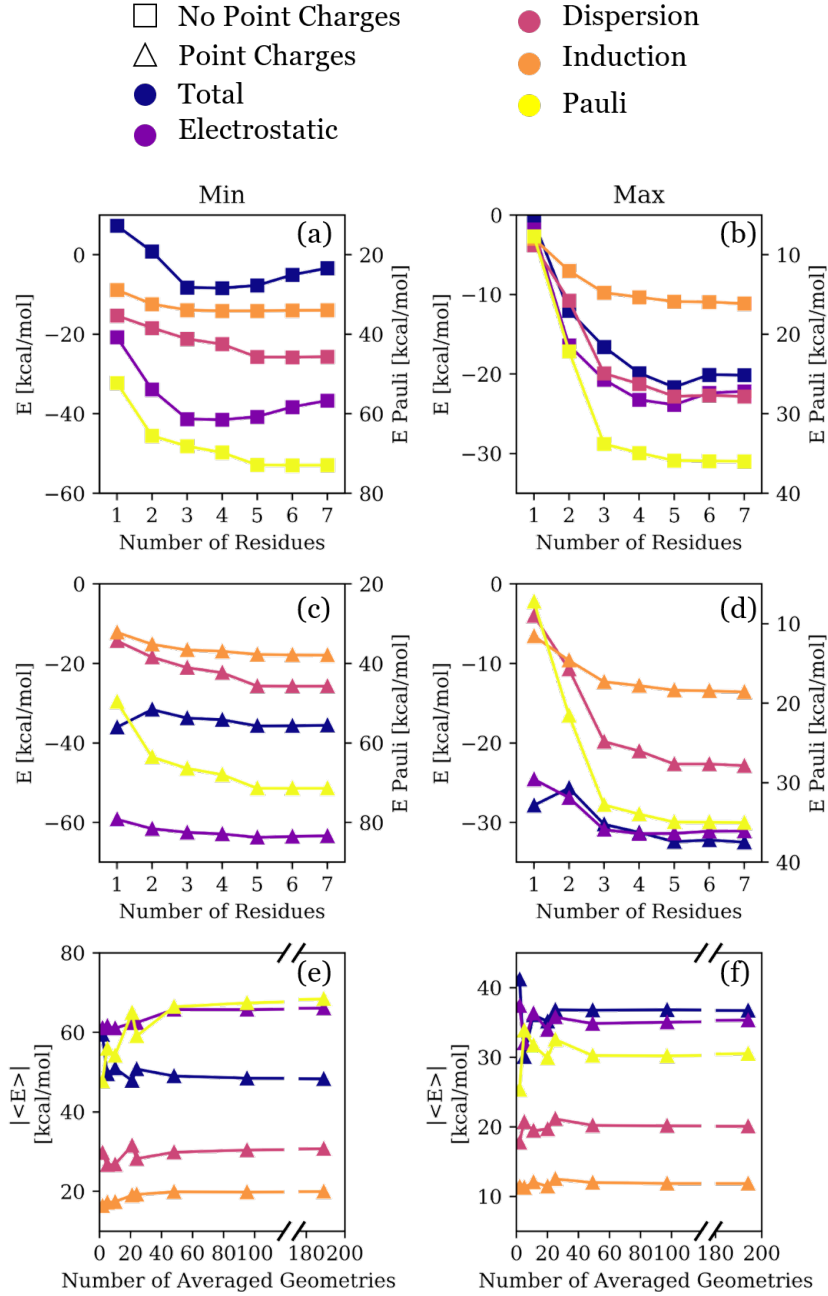
Figure 2: Analysis of the convergence of the interaction energy and the EDA components as the number of DOPC molecules in the QM region increases without (a Min, b Max) and with (c Min, d Max) point charges. Convergence of the absolute value of the interaction energy and the EDA components with respect to the number of (equispaced) geometries considered in the analysis (e Min, f Max).

The probability distributions of the total interaction energies and of each of the energy components that stem from the EDA considering the 190 (194) geometries at Min (Max) are displayed in Figure 3a,c. It is shown that the different energy components are not distributed similarly, but their distributions present different broadness. Furthermore, for both the situation at Min and at Max the broadness of the distribution is seemingly associated with the magnitude of the average value, as can be seen in Figure 3b,d. The total energy and the different energy components present lower average values at Max with respect to the geometries at Min and, therefore, the distributions for the Min region are wider. This is in agreement with the fact that the region of the membrane corresponding to Min is a highly polar and polarizable region, and the interactions between cisplatin and the lipids are stronger than those in the non-polar region (corresponding to Max).

The energy contributions to the interaction energy can be classified into electrostatic and non-electrostatic, the last one corresponding to the sum of dispersion, induction and Pauli repulsion in the present case. In regard with this classification, we observe that at the minimum of the free-energy profile the overall non-electrostatic interactions amount to 17.8 kcal/mol, thus resulting to be repulsive, while the electrostatic contribution is -66.1 kcal/mol (Figure 3b). Therefore, the electrostatic interaction is the main component of the interaction energy; this result is in agreement with the EDA performed considering a classical force field,[30] although it should be emphasized that in the latter case the non-electrostatic component resulted to be attractive, unlike the quantum mechanical analysis performed in this work. Interestingly, when analyzing the averages of the electrostatic and the non-electrostatic components at the center of the membrane (Figure 3d), the electrostatic contribution is still predominant with -35.3 kcal/mol, whereas the non-electrostatic component (albeit being attractive, unlike the minimum) amounts to only -1.4 kcal/mol. These results are in contrast with those previously obtained with a classical force field, for which the non-electrostatic interactions represented the most relevant part of the total interaction energy in the Max region.[30]

All of this can be rationalized by examining the different energy components in terms of attractive (the sum of the electrostatic, dispersion and induction contributions, Figure 3b,d) and repulsive (Pauli) interactions. Specifically, when the relative contributions to the overall attractive energy are analyzed, it can be seen that the electrostatic contribution diminishes from 56.6% to 52.5% from the Min to the Max regions, the dispersion component increases from 26.3% to 29.8%, whereas the induction energy barely increases from 17.1% to 17.6%. These percentages place the electrostatic component as the main attractive contribution in both regions of the membrane, and the fact that the non-electrostatic component (*i.e.*, dispersion + induction + Pauli) varies when going from Min to Max is mainly associated with the decrease in the Pauli repulsive component. These results also suggest that the Pauli repulsion energy is underestimated by the classical force field since the classical non-electrostatic energy resulted to be negative for both the Min and the Max situations.[30] These discrepancies between the classical force field and the present QM/MM analysis indicate that a point-charged force field, although capable of reproducing the experimental free-energy barrier to travel across the bilayer, is not adequate to describe the nature of the interactions that govern the permeation of cisplatin through the lipid membrane.
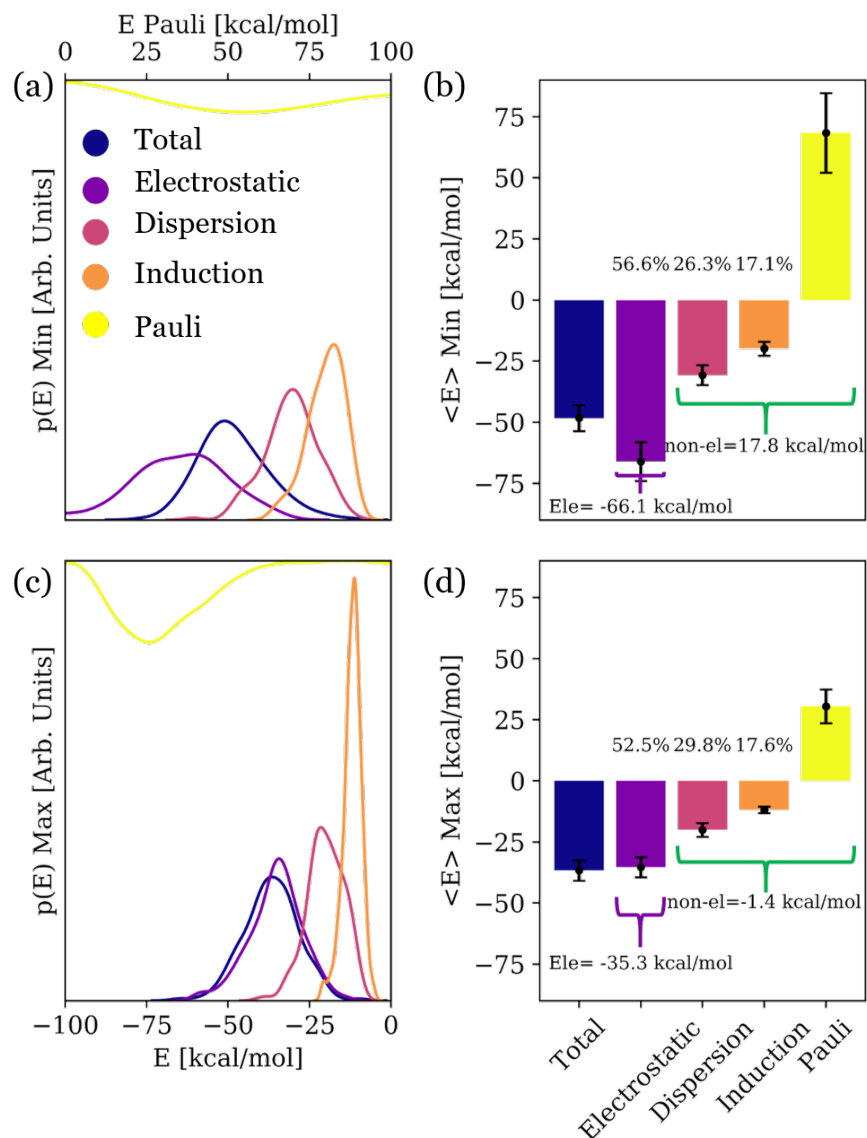
Figure 3: Energy distributions of the contributions to the total interaction energy stemming from the EDA on 190 (194) geometries on a) the minimum (Min) and c) the maximum (Max) of the free-energy profile. Averages and standard deviations of the distributions obtained at Min b) and Max d). The percentages are relative to the overall attractive component to the interaction energy. Electrostatic and non-electrostatic energies (sum of Pauli, induction and dispersion components) are also shown.

It is interesting to analyze which atoms and chemical groups of cisplatin and the DOCP membrane are more relevant for each interaction type. Specifically, we studied the correlation between the value of each energy component and the interatomic distances between cisplatin and the bilayer. It is assumed that these energy terms follow the classical mechanical dependency with the inverse of the interatomic distance $(1/r^n)$. Thus, we have computed the linear correlation coefficient of the electrostatic, induction, dispersion and Pauli energies with respect to $1/r$, $1/r^4$, $1/r^6$ and $1/r^{12}$, respectively. In order to assess the influence of the different functional groups of the DOPC molecule we have divided it into four different moieties, namely, choline, phosphate, glycerol and oleyl. Figure 4 shows the absolute values of the three most prominent correlation coefficients corresponding to the distance between each cisplatin atom type and each atom of the DOPC moieties. The values of the correlation coefficients for all the interatomic distances are listed in the Supporting Information. Noticeably, in the region of the minimum the electrostatic and the induction components present relatively strong correlations (between 0.5 and 0.68) that are spread across the different pairwise interactions between cisplatin and the choline group, indicating a similar participation of these interactions to the overall electrostatic and inductive components. On the other hand, the Pauli component presents a strongly localized correlation (whose coefficient amounts to 0.73) upon the Pt - choline pair, in particular in regard with the distance between the Pt atom and the nitrogen of the choline group (Table S4). The dispersion component of the interaction energy does not show a strong correlation with any pairwise distance, but instead the correlation coefficients are uniformly distributed throughout the four moieties of DOPC, indicating that the dispersion interaction is not dominated by any particular pairwise interaction between cisplatin and DOPC. The situation is different when linear correlations are analyzed at the center of the membrane (Max region), where cisplatin is close the oleyl non-polar tails of the DOPC molecule. It can be concluded from Figure 4 (bottom) that neither of the attractive components of the interaction energy present strong correlations with a specific pairwise distance, unlike in the case of the Min region, where the cisplatin

molecule was surrounded by the polar heads (choline, phosphate and glycol moieties) of the DOPC molecules. This indicates that these energy components are not strongly influenced by any particular pairwise interaction when cisplatin is at the center of the bilayer.
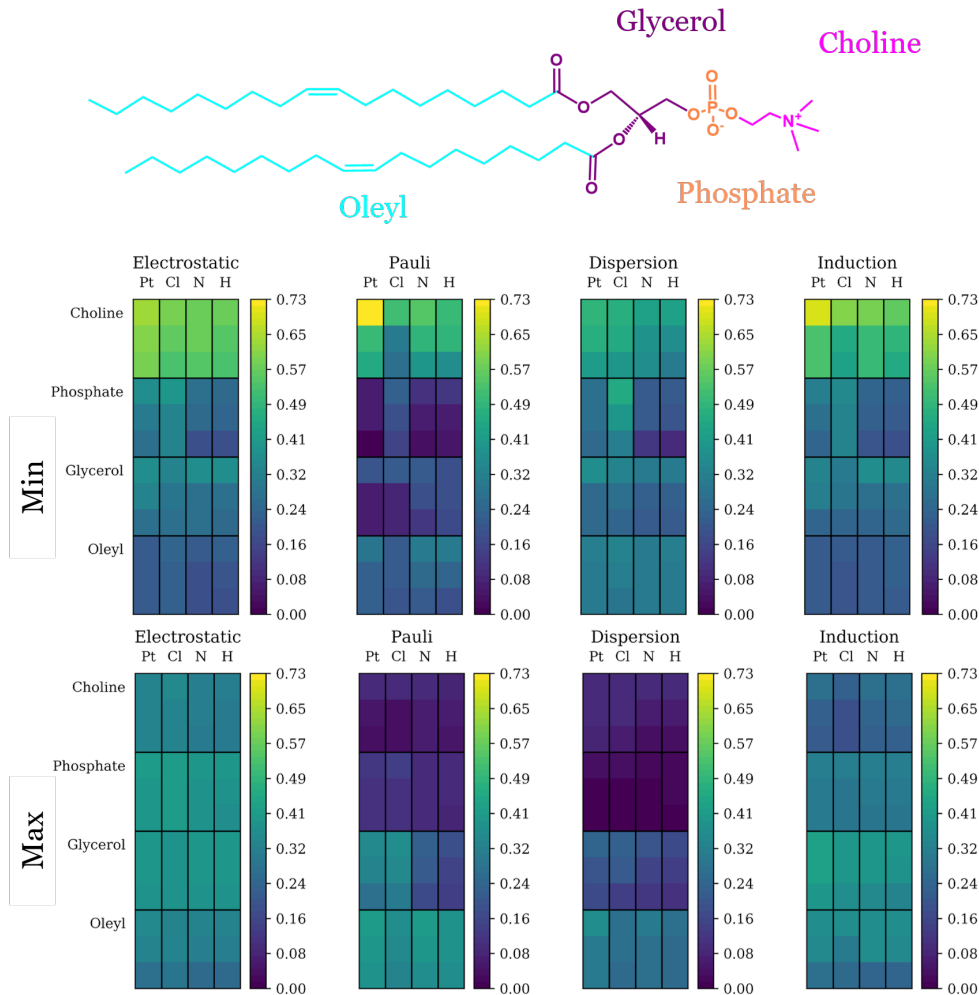

Figure 4: Absolute values of the linear correlation coefficients of the electrostatic, induction, dispersion and Pauli energies with $1/r$, $1/r^4$, $1/r^6$ and $1/r^{12}$, respectively, where all the distances between each cisplatin moiety (Pt, Cl, N, H) and each atom in DOPC are considered, for the Min (top) and the Max (bottom) regions. For each moiety of DOPC (choline, phosphate, glycerol and oleyl) only the three most prominent correlation coefficients are shown.

In conclusion, we have implemented an extension of an EDA scheme based on deformation densities[43,44] to include a multiscale hybrid electrostatic-embedding QM/MM approach. We have applied this methodology to the study of the interaction energy of cisplatin with a DOPC lipid bilayer, whose permeation pathway was previously simulated by umbrella sampling molecular dynamics.[30] We have evidenced the importance of considering a sufficiently large QM region (6 DOPC molecules plus the cisplatin drug), as well as the need of including the surrounding environment within an electrostatic-embedding QM/MM approach to properly compute the interaction energy components. Conformational sampling needs to be accounted for since wide distributions of energies are obtained even when considering sampled geometries from the same region (Min and Max regions). It has been observed that the interaction energy diminishes when moving from the polar to the non-polar region of the bilayer, a fact that is explained by the larger decrease of all the attractive energy components in comparison with the decrease in the Pauli repulsion. Contrary to the classical result,[30] the electrostatic component is predominant in both regions of the membrane, and the Pauli repulsive component plays a major role in determining the overall non-electrostatic component, suggesting that the repulsive component is underestimated by classical force fields. Finally, we have observed that when cisplatin is closer to the polar heads, the electrostatic, induction and Pauli components display strong correlations with the distance between cisplatin and the choline moiety of DOPC, whereas the dispersion energy does not show a strong dependence on a particular distance. At the center of the membrane, when cisplatin is closest to the oleyl moieties, neither of the energy components displays correlations with particular groups. The methodology presented here can be applied to further drug/biomolecule complexes where an accurate characterization of the interactions that govern the system is desired. Moreover, comparison with results based on molecular mechanics force fields will allow the assessment of classical methodologies to describe drug/biomolecule interactions.

Acknowledgement

Supporting Information Available

Working equations of the QM/MM deformation density-based energy decomposition analysis, computational details and correlation coefficients for each energy component at the Min and at the Max regions.

References

(1) Peetla, C.; Stine, A.; Labhasetwar, V. Biophysical interactions with model lipid membranes: Applications in drug discovery and drug delivery. *Mol. Pharm.* **2009**, *6*, 1264–1276.

(2) Zhang, R.; Qin, X.; Kong, F.; Chen, P.; Pan, G. Improving cellular Uptake of Therapeutic Entities through Interaction with Components of Cell Membrane. *Drug Deliv.* **2019**, *26*, 328–342.

(3) Yang, N. J.; Hinner, M. J. Getting Across the Cell Membrane: An Overview for Small Molecules, Peptides, and Proteins. *Methods Mol. Biol.* **2015**, 29–53.

(4) Seddon, A. M.; Casey, D.; Law, R. V.; Gee, A.; Templer, R. H.; Ces, O. Drug Interactions with Lipid Membranes. *Chem. Soc. Rev.* **2009**, *38*, 2509–2519.

(5) Zhang, S.; Lovejoy, K. S.; Shima, J. E.; Lagpacan, L. L.; Shu, Y.; Lapuk, A.; Chen, Y.; Komori, T.; Gray, J. W.; Chen, X.; Lippard, S. J.; Giacomini, K. M. Organic Cation

Transporters Are Determinants of Oxaliplatin Cytotoxicity. *Cancer Res.* **2006**, *66*, 8847–8857.

(6) Johnstone, T. C.; Suntharalingam, K.; Lippard, S. J. The Next Generation of Platinum Drugs: Targeted Pt(II) Agents, Nanoparticle Delivery, and Pt(IV) Prodrugs. *Chem. Rev.* **2016**, *116*, 3436–3486.

(7) Martinho, N.; Santos, T. C. B.; Florindo, H. F.; Silva, L. C. Cisplatin-Membrane Interactions and their Influence on Platinum Complexes Activity and Toxicity. *Front. Physiol.* **2019**, *10*, 1898.

(8) Dilruba, S.; Kalayda, G. V. Platinum-Based Drugs: Past, Present and Future. *Cancer Chemother. Pharmacol.* **2016**, *77*, 1103–1124.

(9) Johnstone, T. C.; Park, G. Y.; Lippard, S. J. Understanding and Improving Platinum Anticancer Drugs - Phenanthriplatin. *Anticancer Res.* **2014**, *34*, 471–476.

(10) Czapla-Masztafiak, J.; Nogueira, J. J.; Lipiec, E.; Kwiatek, W. M.; Wood, B. R.; Deacon, G. B.; Kayser, Y.; Fernandes, D. L. A.; Pavliuk, M. V.; Szlachetko, J.; González, L.; Sá, J. Direct Determination of Metal Complexes' Interaction with DNA by Atomic Telemetry and Multiscale Molecular Dynamics. *J. Phys. Chem. Lett.* **2017**, *8*, 805–811.

(11) Chen, Q.; Yang, Y.; Lin, X.; Ma, W.; Chen, G.; Li, W.; Wang, X.; Yu, Z. Platinum(IV) Prodrugs with Long Lipid Chains for Drug Delivery and Overcoming Cisplatin Resistance. *Chem. Comm.* **2018**, *54*, 5369–5372.

(12) Veclani, D.; Melchior, A.; Tolazzi, M.; Cerón-Carrasco, J. P. Using Theory to Reinterpret the Kinetics of Monofunctional Platinum Anticancer Drugs: Stacking Matters. *J. Am. Chem. Soc.* **2018**, *140*, 14024–14027.

(13) Ramachandran, S.; Temple, B.; Alexandrova, A. N.; Chaney, S. G.; Dokholyan, N. V.

Recognition of Platinum-DNA Adducts by HMGB1a. *Biochemistry* **2012**, *51*, 7608–7617.

(14) Smith, I. E.; Talbot, D. C. Cisplatin and its Analogues in the Treatment of Advanced Breast Cancer: a Review. *Br. J. Cancer* **1992**, *65*, 787–793.

(15) Barabas, K.; Milner, R.; Lurie, D.; Adin, C. Cisplatin: a Review of Toxicities and Therapeutic Applications. *Vet. Comp. Oncol.* **2008**, *6*, 1–18.

(16) Dasari, S.; Bernard Tchounwou, P. Cisplatin in Cancer Therapy: Molecular Mechanisms of Action. *Eur. J. Pharmacol.* **2014**, *740*, 364–378.

(17) Ho, G. Y.; Woodward, N.; Coward, J. I. Cisplatin Versus Carboplatin: Comparative Review of Therapeutic Management in Solid Malignancies. *Crit. Rev. Oncol. Hematol.* **2016**, *102*, 37–46.

(18) Eljack, N. D.; Ma, H. Y. M.; Drucker, J.; Shen, C.; Hambley, T. W.; New, E. J.; Friedrich, T.; Clarke, R. J. Mechanisms of Cell Uptake and Toxicity of the Anticancer Drug Cisplatin. *Metallomics* **2014**, *6*, 2126–2133.

(19) Chen, S. H.; Chang, J. Y. New Insights into Mechanisms of Cisplatin Resistance: From Tumor Cell to Microenvironment. *Int. J. Mol. Sci.* **2019**, *20*, 4136.

(20) Rebillard, A.; Tekpli, X.; Meurette, O.; Sergent, O.; LeMoigne-Muller, G.; Vernhet, L.; Gorria, M.; Chevanne, M.; Christmann, M.; Kaina, B.; Counillon, L.; Gulbins, E.; Lagadic-Gossmann, D.; Dimanche-Boitrel, M. T. Cisplatin-Induced Apoptosis Involves Membrane Fluidification via Inhibition of NHE1 in Human Colon Cancer Cells. *Cancer Res.* **2007**, *67*, 7865–7874.

(21) Neale, C.; Hsu, J.; Yip, C.; Pomès, R. Indolicidin Binding Induces Thinning of a Lipid Bilayer. *Biophys. J.* **2014**, *106*, L29–L31.

(22) Filipe, H. A. L.; Moreno, M. J.; Róg, T.; Vattulainen, I.; Loura, L. M. S. How To Tackle the Issues in Free Energy Simulations of Long Amphiphiles Interacting with Lipid Membranes: Convergence and Local Membrane Deformations. *J. Phys. Chem. B* **2014**, *118*, 3572–3581.

(23) Nogueira, J. J.; Meixner, M.; Bittermann, M.; González, L. Impact of Lipid Environment on Photodamage Activation of Methylene Blue. *ChemPhotoChem* **2017**, *1*, 178–182.

(24) Sánchez-Murcia, P. A.; Nogueira, J. J.; González, L. Exciton Localization on Ru-Based Photosensitizers Induced by Binding to Lipid Membranes. *J. Phys. Chem. Lett.* **2018**, *9*, 683–688.

(25) Bochicchio, D.; Panizon, E.; Ferrando, R.; Monticelli, L.; Rossi, G. Calculating the Free Energy of Transfer of Small Solutes into a Model Lipid Membrane: Comparison between Metadynamics and Umbrella Sampling. *J. Chem. Phys.* **2015**, *143*.

(26) Neale, C.; Pomès, R. Sampling Errors in Free Energy Simulations of Small Molecules in Lipid Bilayers. *Biochim. Biophys. Acta* **2016**, *1858*, 2539–2548.

(27) Yesylevskyy, S.; Cardey, B.; Kraszewski, S.; Foley, S.; Enescu, M.; da Silva, A. M.; Santos, H. F. D.; Ramseyer, C. Empirical Force Field for Cisplatin Based on Quantum Dynamics Data: Case Study of New Parameterization Scheme for Coordination Compounds. *J. Mol. Model.* **2015**, *21*, 268.

(28) Rivel, T.; Ramseyer, C.; Yesylevskyy, S. The Asymmetry of Plasma Membranes and their Cholesterol Content Influence the Uptake of Cisplatin. *Sci. Rep.* **2019**, *9*, 5627.

(29) Yesylevskyy, S.; Rivel, T.; Ramseyer, C. Curvature Increases Permeability of the Plasma Membrane for Ions, Water and the Anti-Cancer Drugs Cisplatin and Gemcitabine. *Sci. Rep.* **2019**, *9*, 17214.

(30) Ruano, L.; Cárdenas, G.; Nogueira, J. J. The Permeation Mechanism of Cisplatin through a Dioleoylphosphocholine Bilayer. *ChemPhysChem* **2021**, *22*, 1–12.

(31) Morokuma, K. Molecular Orbital Studies of Hydrogen Bonds. III. C=O···H–O Hydrogen Bond in H2CO···H2O and H2CO···2H2O. *J. Chem. Phys.* **1971**, *55*, 1236–1244.

(32) Phipps, M. J. S.; Fox, T.; Tautermann, C. S.; Skylaris, C. K. Energy Decomposition Analysis Approaches and Their Evaluation on Prototypical Protein-Drug Interaction Patterns. *Chem. Soc. Rev.* **2015**, *44*, 3177–3211.

(33) Zhao, L.; von Hopffgarten, M.; Andrada, D. M.; Frenking, G. Energy Decomposition Analysis. *WIREs Comput. Mol. Sci.* **2018**, *8*, e1345.

(34) Jeziorski, B.; Moszynski, R.; Szalewicz, K. Perturbation Theory Approach to Intermolecular Potential Energy Surfaces of van der Waals Complexes. *Chem. Rev.* **1994**, *94*, 1887–1930.

(35) Lao, K. U.; Herbert, J. M. Accurate Intermolecular Interactions at Dramatically Reduced Cost: XPol+SAPT with Empirical Dispersion. *J. Phys. Chem. Lett.* **2012**, *3*, 3241–3248.

(36) Mao, Y.; Horn, P. R.; Head-Gordon, M. Energy Decomposition Analysis in an Adiabatic Picture. *Phys. Chem. Chem. Phys.* **2017**, *19*, 5944–5958.

(37) Mao, Y.; Head-Gordon, M. Probing Blue-Shifting Hydrogen Bonds with Adiabatic Energy Decomposition Analysis. *J. Phys. Chem. Lett.* **2019**, *10*, 3899–3905.

(38) Calle-Vallejo, F.; Sautet, P.; Loffreda, D. Understanding Adsorption-Induced Effects on Platinum Nanoparticles: An Energy-Decomposition Analysis. *J. Phys. Chem. Lett.* **2014**, *5*, 3120–3124.

(39) Carballeira, D. L.; Ramos-Berdullas, N.; Pérez-Juste, I.; Fajín, J. L. C.; Cordeiro, M. N.

D. S.; Mandado, M. A Computational Study of the Interaction of Graphene Structures with Biomolecular Units. *Phys. Chem. Chem. Phys.* **2016**, *18*, 15312–15321.

(40) Bamdad, M.; Farrokhpour, H.; Najafi, B.; Ashrafizaadeh, M. Energy Decomposition Analysis of the Intermolecular Interaction Energy between Different Gas Molecules (H2, O2, H2O, N2, CO2, H2S, and CO) and Selected Li+-Doped Graphitic Molecules: DF-SAPT (DFT) Calculations. *Theor. Chem. Acc.* **2018**, *137*.

(41) Carter-Fenk, K.; Lao, K. U.; Liu, K.-Y.; Herbert, J. M. Accurate and Efficient ab Initio Calculations for Supramolecular Complexes: Symmetry-Adapted Perturbation Theory with Many-Body Dispersion. *J. Phys. Chem. Lett.* **2019**, *10*, 2706–2714.

(42) Boys, S.; Bernardi, F. The Calculation of Small Molecular Interactions by the Differences of Separate Total Energies. Some Procedures With Reduced Errors. *Mol. Phys.* **1970**, *19*, 553–566.

(43) Mandado, M.; Hermida-Ramón, J. M. Electron Density Based Partitioning Scheme of Interaction Energies. *J. Chem. Theory Comput.* **2011**, *7*, 633–641.

(44) Ramos-Berdullas, N.; Pérez-Juste, I.; Van Alsenoy, C.; Mandado, M. Theoretical Study of the Adsorption of Aromatic Units on Carbon Allotropes Including Explicit (Empirical) DFT Dispersion Corrections and Implicitly Dispersion-Corrected Functionals: The Pyridine Case. *Phys. Chem. Chem. Phys.* **2015**, *17*, 575–587.